the last decade (Schuster and Watson 2007; Thomas et al. 2008). The largest increases in anthropogenic carbon accumulation along these sections appear to be in the Southern Hemisphere oceans.

Figure 3.28 shows the change in carbon column inventories between the CLIVAR (2008), WOCE (1995), and GEOSECS (1978) cruises in the eastern Indian Ocean along 90°E. The pattern of average annual carbon increases between 1995 and 2008 were similar to the pattern of increases between 1978 and 1995, but the magnitude of the increases over the last decade are about twice the increases prior to 1995. These findings appear to contradict some recently published model results and surface ocean pCO_2 observations that have suggested that the Southern Ocean uptake of CO_2 has decreased over the last few decades (Le Quéré et al. 2007; Lovenduski et al. 2007; Takahashi et al. 2009). There are still more lines that need to be examined in the Southern Ocean, but these initial results illustrate the importance of studying the linkages and differences between CO_2 uptake from the atmosphere and the ultimate storage of carbon in the ocean interior.

Because atmospheric CO_2 concentrations are growing at a nearly exponential rate, it is not surprising to find that the rate of carbon storage is increasing with time. However, there are two processes that control the rate of anthropogenic carbon increases in the ocean: the equilibration time between the ocean and the atmosphere and the rate at which waters containing anthropogenic carbon are moved into the ocean's interior. In most places the surface ocean CO_2 values are increasing at roughly the same rate as the atmosphere (Takahashi et al. 2009). This means that anthropogenic CO_2 is accumulating in surface waters everywhere at approximately the same rate. There are only a few locations, however, where surface waters are moving into the ocean interior.

North of about 55°S the difference between the two curves in Fig. 3.28 is reasonably consistent. Because both curves show the largest overall accumulations of carbon in the southern subtropical gyre, the percent change in the carbon accumulation rate is much larger north of 10°S (from 0.2–0.3 to ~0.6 mol m^{-2} yr^{-1}, or roughly a 100% increase) compared to the region south of approximately 10°S (from 0.7–0.9 to 1.0–1.2 mol m^{-2} yr^{-1}, or about a 30% increase). This observation is consistent with the idea that surface layer accumulation of anthropogenic carbon has increased at all latitudes, but the rate of transport of anthropogenic carbon into the ocean interior has not changed dramatically along this section. The anthropogenic carbon penetration is still relatively shallow north of 10°S, thus the increase in surface uptake resulted in a significant increase in the total carbon column inventory. South of 10°S, however, much of the anthropogenic carbon is found in the intermediate waters. An increase in the surface accumulation rate without a subsequent increase in the rate at which CO_2 is moved into the ocean interior, therefore, would result in a smaller percent increase in the total column inventory as observed.

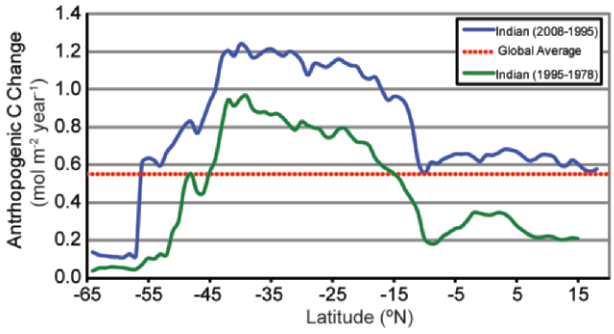

Fig. 3.28. Column Inventory changes as a function of latitude along ~90°E in the eastern Indian Ocean. The blue line is the average annual change between 2007 and 1995. The green line is the average annual change between 1995 and 1978. The red dotted line is the global-average annual uptake of anthropogenic CO_2 divided by the surface area of the ocean.

These latest results show conclusively that anthropogenic CO_2 is continuing to accumulate in the Atlantic, Pacific, and Indian Oceans and suggest that the accumulation rates can vary over decadal time scales. However, a single transect through an ocean basin is not sufficient for characterizing the full patterns of anthropogenic CO_2 storage. More in-depth analyses will be undertaken once the global survey is complete. Because circulation and biological processes changes can vary in cycles often associated with ocean climate reorganizations such as ENSO, North Atlantic Oscillation, Pacific decadal oscillation, and southern annular mode, it is critical to continue to monitor the changes in carbon inventories and how they interact with the secular increases in anthropogenic CO_2.

k. Global ocean phytoplankton—M. J. Behrenfeld, D. A. Siegel, R. T. O'Malley, and S. Maritorena

Photosynthesis by the free-floating, single-celled phytoplankton of the upper sunlit "photic" layer of the global ocean is the overwhelmingly dominant source of organic matter fueling marine ecosystems. Phytoplankton contribute roughly half of annual biospheric (i.e., terrestrial and aquatic) NPP (gross photosynthesis minus plant respiration), and their

NEW EVIDENCE FOR OCEAN ACIDIFICATION IN COASTAL WATERS OF NORTH AMERICA—R. A. FEELY AND A. G. DICKSON

Over the past two centuries the release of CO_2 from humankind's combined industrial and agricultural practices has resulted in atmospheric CO_2 concentrations that are now higher than experienced on the Earth for at least the last 800,000 years (Lüthi et al. 2008). During this period the oceans have taken up approximately one-third of the total amount of CO_2 produced by human activities (Sabine et al. 2004). This addition of anthropogenic CO_2 to the ocean has reduced the surface ocean pH by about 0.1 to date (a process known as ocean acidification) and is expected to reduce pH by a further 0.3 units by the end of this century (Feely et al. 2004). It now appears likely that the level of CO_2 in the atmosphere might double over its preindustrial levels by the middle of this century. This rapid change in ocean chemistry is more dramatic than at any time in the past 20 million years (Feely et al. 2004). This pH decrease will lead to a reduction in the saturation state of seawater with respect to calcite and aragonite, which are the two most common types of calcium carbonate formed by marine organisms (Feely et al. 2004). These changes in seawater chemistry have consequences for a wide variety of marine organisms in coastal and open ocean ecosystems. Many species of marine calcifiers, such as clams, oysters, mussels, sea urchins, and corals, have exhibited reduced calcification rates in response to elevated CO_2 levels (Kleypas et al. 2006; Fabry et al. 2008; Doney et al. 2009). On the other hand, other noncalcifying species, including sea grasses (Palacios and Zimmermann 2007; Hall-Spencer et al. 2008), and nitrogen-fixing bacteria (Hutchins et al. 2007) appear to produce increased biomass under increased CO_2 levels.

Recent studies have provided new findings that organisms growing in estuaries or in coastal upwelling zones, such as near river mouths or along the continental shelf of the west coast of North America, may already be experiencing significant biological effects resulting from the combined impacts of freshwater input, coastal upwelling, and ocean acidification (Salisbury et al. 2008; Feely et al. 2008). For example, Salisbury et al. (2008) demonstrated that discharge of acidic river water over the continental shelf may result in poor conditions for shell formation. When the low-alkalinity river water mixes into the surface ocean it can significantly reduce the aragonite or calcite saturation state. For many rivers, this process could inhibit the development of certain shellfish larvae such as the commercially valuable clam Mya arenaria.

On the west coast of North America, the seasonal upwelling of subsurface waters along the coast brings CO_2-enriched waters onto the shelf and, in some instances, into the surface ocean (Fig. 3.29). It appears that this water, in addition to its original high level of CO_2 resulting from natural respiration processes in the subsurface layers, is also significantly contaminated with anthropogenic CO_2 as it was last in contact with the atmosphere about 50 years ago when it took up additional CO_2 from the atmosphere. An immediate consequence of this additional CO_2 is that the CO_2 concentrations in these upwelled waters will be significantly greater than they would have been in preindustrial times. Furthermore, each ensuing year will draw on water that has been exposed to the atmosphere still more recently, resulting in yet higher CO_2 levels. Because these "ocean-acidified" upwelled waters are undersaturated with respect to aragonite, they are already a potential threat to many of the calcifying aragonitic species that live along such coasts.

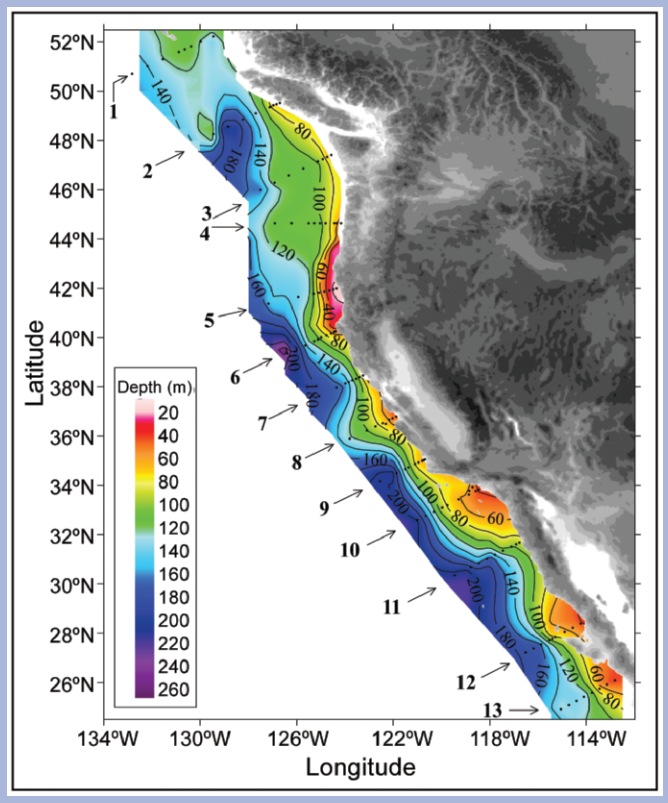

FIG. 3.29 (after Feely et al. 2008). Distribution of the depths of "ocean acidified" undersaturated water (aragonite saturation <1.0; pH <7.75) on the continental shelf of western North America from Queen Charlotte Sound, Canada, to San Gregorio Baja California Sur, Mexico. On transect line 5, the corrosive water reaches all the way to the surface in the inshore waters near the coast. The black dots represent station locations.

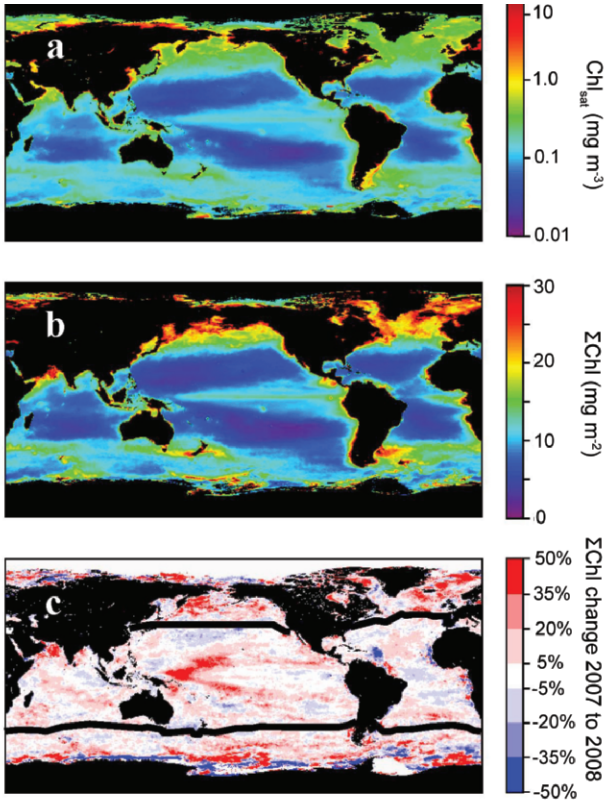

FIG. 3.30. (a) Average MODIS–*Aqua* Chl_{sat} for 2008. (b) Average MODIS-*Aqua* ΣChl for 2008. (c) Percentage change in ΣChl from 2007 to 2008. Heavy black lines demark permanently stratified oceans (2007 average SST >15°C) from higher-latitude regions (2007 average SST < 15°C). Because data were only available through day 320 of 2008 at the time of our analysis, here and in the main text annual values are for Julian dates 321 of a given year to 320 of the following year (e.g., the 2008 period = Julian day 321, 2007 to Julian day 320, 2008). Photic zone chlorophyll content calculated following Behrenfeld et al. (2006).

photosynthetic carbon fixation is the primary conduit through which atmospheric CO_2 is transferred into ocean organic carbon pools. Thus, these tiny suspended ocean "plants" play a vital role in world fisheries and the Earth's biogeochemical cycles.

The productivity of phytoplankton depends on the availability of sunlight, macronutrients (e.g., nitrogen, phosphorous), and micronutrients (e.g., iron), and thus is sensitive to climate-driven changes in these resources. Since 1997, a continuous satellite record of global climate-quality ocean color data has existed, allowing quantification of phytoplankton properties and investigation of broad relationships between upper-ocean environmental conditions and biology (e.g., McClain 2009). The ecosystem property most often derived from ocean color observations is the surface chlorophyll concentration (Chl_{sat}) (Fig. 3.30a), which can be taken as representative of the upper mixed layer and is a complex expression of phytoplankton standing stock (biomass) and physiological responses to prevailing light and nutrient levels. Chl_{sat} varies globally by three orders of magnitude (roughly 0.03 to >30 mg m^{-3}). A relevant property for ocean biology and biogeochemistry is the chlorophyll standing stock integrated over the photic zone (ΣChl; e.g., Behrenfeld et al. 2006), where the photic zone is traditionally defined as the layer between the surface and 1% light depth. Qualitatively, ΣChl exhibits a similar global distribution as Chl_{sat} (Fig. 3.30b), but ΣChl is roughly proportional to the square root of Chl_{sat}, so its value range is constrained to only 1.3 orders of magnitude (Behrenfeld et al. 2008a; Behrenfeld and Falkowski 1997).

Since the beginning of the satellite ocean color record, a striking correspondence has emerged between global variations in ΣChl and SST (Gregg et al. 2005; Behrenfeld et al. 2006). In 2008, our ability to monitor, refine, and interpret this relationship weakened. For the past decade, the SeaWiFS provided an unbroken time series of well-characterized global ocean data, but multiple satellite system failures this past year yielded temporal discontinuities in the record, with data gaps extending several months. Consequently, continuation of the long-term satellite record requires merging SeaWiFS data with products from the MODIS on the *Aqua* EOS satellite, which unavoidably introduces a potential for intersensor artifacts in the time series. Data from the MODIS sensor on the *Terra* EOS satellite are not used because the MODIS–*Terra* sensor has many technical issues that limit its utility for climate applications (e.g., Kwiatkowska et al. 2008).

SeaWiFS and MODIS–*Aqua* observations overlap continuously between July 2002 and December 2007. Over this 66-month period, global-average Chl_{sat} for SeaWiFS is 0.302 mg m^{-3}, average photic zone chlorophyll (ΣChl) is 13.5 mg m^{-2}, and total global chlorophyll standing stock for the photic zone averages 4.6 Tg. Sixty-one percent of this global chlorophyll stock is found in the permanently stratified oceans (approximated here as waters with annual average SST in 2007 of >15°C), which cover 72% of the ocean surface. The remaining 39% of global chlorophyll stock is found in the more productive seasonal seas at higher latitudes. By comparison, MODIS–*Aqua* data for the same 66-month period give a global-average Chl_{sat} of 0.266 mg m^{-3}, an average ΣChl of 12.1 mg m^{-2}, and an average global chlorophyll stock of 4.1 Tg, with 62% of this stock found in the

permanently stratified oceans. The elevated values of chlorophyll for SeaWiFS relative to MODIS–*Aqua* reflect a persistent bias between the two datasets, as clearly seen in the time series of monthly chlorophyll stocks for the permanently stratified oceans (Fig. 3.31a). On average, SeaWiFS chlorophyll values are 13.2% higher than MODIS–*Aqua*. When applied to the Vertically Generalized Production Model (Behrenfeld and Falkowski 1997), SeaWiFS data yield annual ocean NPP estimates ranging from 51.2 to 52.3 Pg C y^{-1}, while MODIS-*Aqua* gives values of 45.6 to 46.9 Pg C y^{-1} (average intersensor bias between NPP values is 12.3%).

Sensor gains for SeaWiFS and MODIS–*Aqua* are determined through comparison with the same in situ dataset (e.g., Franz et al. 2007), but no deliberate effort has been specifically made to date to minimize discrepancies between the resulting satellite data products. In 2009, both datasets will undergo a complete reprocessing, after which issues of bias between the two sensors should be reevaluated.

For 2008, the complete annual record provided by MODIS–*Aqua* gives an average Chl_{sat} of 0.271 mg m^{-3} and an average ΣChl of 12.4 mg m^{-2}. While the MODIS–*Aqua* globally integrated chlorophyll standing stock for 2008 of 4.1 Tg is only 1.4% higher than the 2007 value, regional changes in ΣChl were substantial and ranged to ±50% (Fig. 3.30c). Pixel-level comparison of these ΣChl changes with coincident changes in MODIS–*Aqua* SST data yields an inverse relationship for 66% of the stratified ocean (i.e., ΣChl decreases with increasing SST, and vise versa), while only 34% of the region exhibits a positive correlation. This result can be viewed in the broader context of the full satellite record by merging SeaWiFS, MODIS–*Aqua*, and AVHRR data and comparing monthly chlorophyll and SST anomalies for the permanently stratified, northern high-latitude, and southern high-latitude zones.

Monthly chlorophyll anomalies for the stratified oceans exhibit a remarkable coherence between the two records (r^2 = 0.81) (Fig. 3.31b), despite the bias between SeaWiFS and MODIS–*Aqua* data (e.g., Fig. 3.31a). Similar intersensor agreement in chlorophyll anomalies is also found for the two high-latitude zones (i.e., annual average SST <15°C). While these results do not diminish the impact of SeaWiFS/MODIS–*Aqua* biases on quantitative analyses of phytoplankton standing stocks and rates, they do imply that anomaly trends can be evaluated across the merged dataset. With respect to SST and in contrast to chlorophyll, AVHRR and MODIS–*Aqua* data for the 2002–07 period do not show significant intersensor

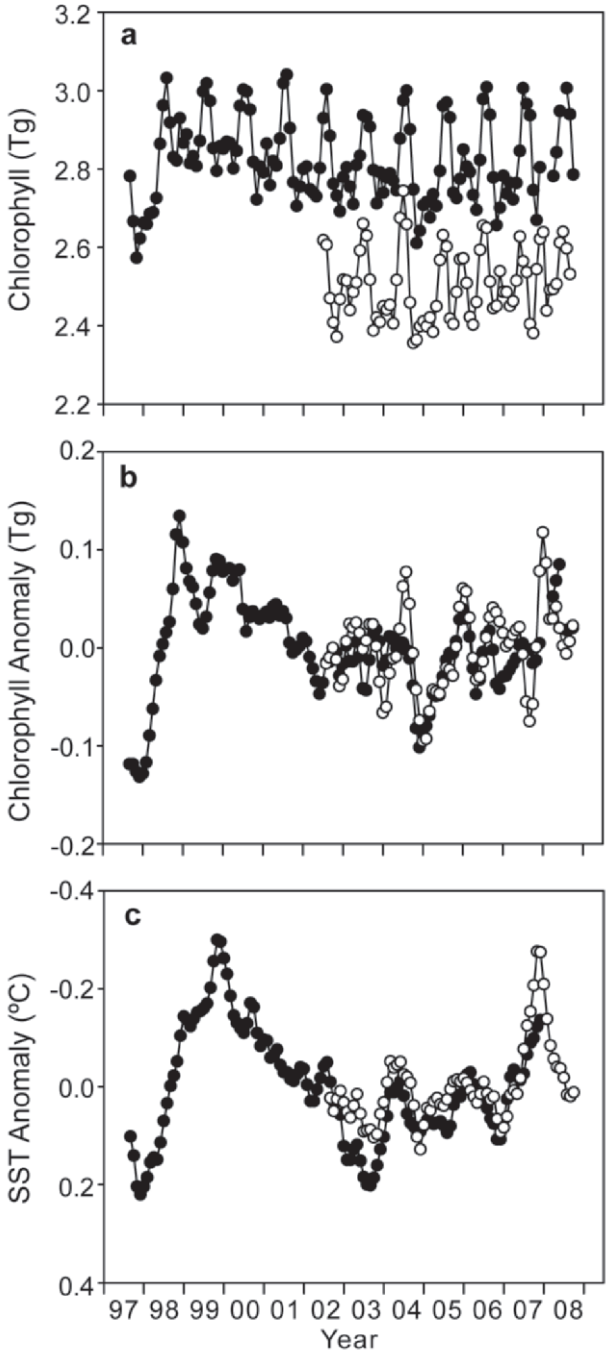

Fig. 3.31. (a) Monthly photic zone chlorophyll concentrations (= average ΣChl times area) for the permanently stratified oceans (SST >15°C; Fig. 1c). Solid symbols are SeaWiFS data. Open symbols are MODIS–*Aqua* data. (b) Monthly anomalies in stratified ocean photic zone chlorophyll for SeaWiFS (solid symbols) and MODIS–*Aqua* (open symbols). Anomalies represent the difference between photic zone chlorophyll for a given month and the average value for that month for a given sensor record. (c) Monthly anomalies in mean SST for the stratified oceans based on AVHRR-quality 5–8 data (solid symbols) and MODIS SST4 data (open symbols).

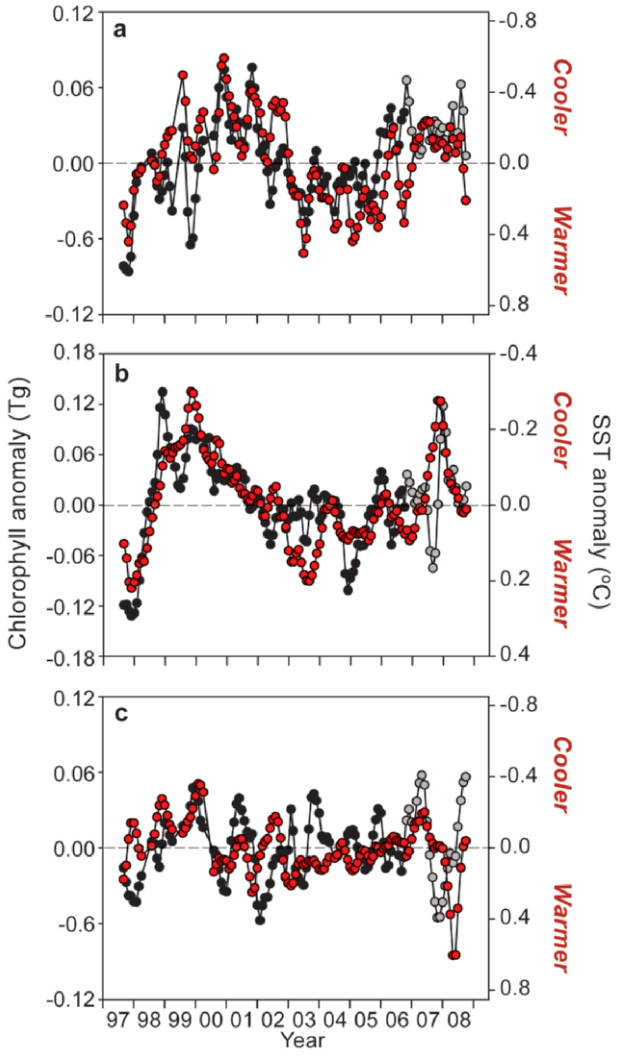

Fig. 3.32. Comparison of monthly anomalies in photic zone chlorophyll (black and gray symbols, left axis) and SST (red symbols, right axis). (a) Northern waters with 2007 average SST < 15°C. (b) Permanently stratified waters with 2007 average SST > 15°C. (c) Southern waters with 2007 average SST < 15°C. (a–c) Solid black symbols are SeaWiFS data. Gray symbols are MODIS–*Aqua* data. MODIS–*Aqua* data are spliced into the SeaWiFS record beginning on Julian day 321, 2006, to be consistent with Fig. 1. Horizontal dashed line in each panel corresponds to monthly climatological average values. (Note, left axes increase from bottom to top, while right axes decrease from bottom to top.)

biases and their SST anomalies are highly correlated ($r^2 = 0.91$) (Fig. 3.31c).

From the merged datasets, we find that the chlorophyll–SST relationship observed during 2008 is consistent with longer-term patterns observed since the first SeaWiFS images in September 1997 (Fig. 3.32). At northern high latitudes, oscillations in monthly chlorophyll anomalies are inversely correlated with SST anomalies (linear regression slope $p < 0.01$) (Fig. 3.32a). Note that the SST anomaly scale in all panels of Fig. 3.32 is the right-hand axes, with cooling at the top and warming at the bottom (as in Fig. 3.31c). Similarly, chlorophyll and SST anomalies are inversely related in the permanently stratified oceans (linear regression slope $p < 0.001$) (Fig. 3.32b). At high southern latitudes, weaker temporal trends in chlorophyll and SST are found, but an inverse relationship is still apparent and significant (linear regression slope $p < 0.05$). Combining the two polar regions, we find that the slope of the chlorophyll–SST relationship is a factor of 3 steeper (i.e., greater change in chlorophyll per unit change in SST) than in the permanently stratified zone.

Despite all three of our global zones exhibiting inverse chlorophyll–SST relationships, it is important to recognize their correlative, not causative, underpinnings. Ninety percent of the SST anomalies shown in Fig. 3.32 are within ±0.3°C of the 11-yr record monthly mean values (s.d. = 0.11°C), and the full range of anomaly values barely span a 1°C range. The direct physiological consequences (e.g., enzymatic reaction rates) of such minute temperature changes are negligible. Thus, correlations between SST and chlorophyll anomalies emerge because SST acts as a surrogate for other environmental factors that vary with SST and directly impact phytoplankton chlorophyll levels. Two such factors are nutrients (including iron) and mixed layer light levels. In general, surface layer warming is associated with stronger surface layer stratification and shallower mixing depths, which in turn increase average mixed layer phytoplankton light exposure and can hamper vertical nutrient exchange (Behrenfeld et al. 2005; Siegel et al. 2005). Decreased nutrient availability suppresses phytoplankton cellular chlorophyll levels and can diminish phytoplankton biomass. Likewise, acclimation to enhanced mixed layer light exposure entails reductions in cellular chlorophyll. Changes in seasonal surface mixing cycles can also influence chlorophyll levels by altering predator–prey interactions and thereby phytoplankton biomass and species composition. Thus, it is the correlation between SST and the summed expression of these direct nutrient, light, and ecosystem effects that gives rise to inverse chlorophyll–SST relationships. The relative importance of these controlling factors, however, varies over space and time (e.g., Behrenfeld et al. 2008b) and is expressed through variations in the slope of the chlorophyll–SST relationship.

Conclusions of the 2008 analysis are that 1) continuation of the satellite-based climate record for

global chlorophyll anomalies was possible, despite prolonged 2008 gaps in SeaWiFS data, because of a substantial and continuous overlap period between SeaWiFS and MODIS–*Aqua* observations; 2) the rise in chlorophyll for the stratified oceans between 2007 and 2008 corresponds with an ENSO shift toward La Niña conditions; 3) net inverse relationships between anomalies in chlorophyll and SST for the merged data are consistent with SeaWiFS-only trends since 1997; 4) intersensor biases in ocean products, while not preventing extension of anomaly trends, do have a significant impact on quantitative assessments of global chlorophyll concentrations and NPP; and 5) continuity of satellite ocean color observations is essential for understanding global ocean biosphere changes and feedbacks (Siegel et al. 2008).